Available online at www.sciencedirect.com

ScienceDirect

Energy Procedia 57 (2014) 1120 – 1129

Energy Procedia

2013 ISES Solar World Congress

Distribution of solar diffuse fraction in Taiwan

Chia-Wei Kuo[a], Wen-Chey Chang[a], Keh-Chin Chang[b,]*

[a]*Energy Research Center, National Cheng Kung University, No.2500, Sec.1., Zhongzheng S. Rd., Guiren Dist., Tainan 71150, Taiwan*

[b]*Department of Aeronautics and Astronautics, National Cheng Kung University, No.1, Daxue Rd., East Dist., Tainan 701, Taiwan*

Abstract

A simple polynomial model of the sky clearness index as predictor was proposed in this paper, for estimating the hourly solar diffuse fractions in Taiwan. The error analysis was performed through two statistical indicators, the mean bias error and the root-mean-square error. The out of database validation was also made to confirm the model generality. Next, regressions between monthly averaged conditions and geographical parameters of places (latitude, longitude, and elevation above sea level) were discussed, using the model's estimates and the updated data sets of typical solar radiation year. Based on the results, diffuse fraction maps for two observation periods were presented in 1-km resolution via an aid of linear interpolation.

Selection and/or peer-review under responsibility of ISES.

Keywords: diffuse fraction; typical solar radiation year; solar energy; model assessment

1. Introduction

The concentrating solar thermal systems such as central receivers, parabolic troughs, or paraboloidal dishes, were competitive in high temperature solar thermal applications as allowing the highest possible energy collection. In this case, the system efficiency was strongly affected by solar diffuse fraction (*d*), in which a higher value would give a lower performance. Thus, to well calculate thermal load of end users and size of collector by concentrating means, a good knowledge about diffuse fraction distributions was important.

* Corresponding author. Tel.: +886-6-2757575 ext. 63679; fax: +886-6-2389940.
E-mail address: kcchang@mail.ncku.edu.tw.

Selection and/or peer-review under responsibility of ISES.
doi:10.1016/j.egypro.2014.10.098

$$d = \frac{I_{diffuse}}{I_{global}} \quad (1)$$

The direct data collections at many places were not practical since $I_{diffuse}$ records were not provided in reports of the Taiwan Central Weather Bureau. Consequently, a simple polynomial model which could provide hourly estimates was needed. Next, the updated typical solar radiation years (TSRY) which had 20 major meteorological stations for the 2002 – 2011 I_{global} records were established. It was aimed to give representative data sets in finding the best regressions between monthly diffuse fractions and geographical parameters of places (latitude, longitude, and elevation above sea level). The results could then be applied to build maps showing distributions.

Nomenclature

d	hourly horizontal diffuse fraction
d_{est}	estimated hourly horizontal diffuse fraction
d_{mea}	measured hourly horizontal diffuse fraction
$\overline{d_{mea}}$	mean of d_{mea}
H_o	hourly extraterrestrial radiation (kJ/hr.m^2)
h	elevation above sea level (km)
$I_{diffuse}$	hourly horizontal diffuse radiation (kJ/hr.m^2)
I_{global}	hourly horizontal global radiation (kJ/hr.m^2)
k_t	hourly sky clearness index
MABE	mean absolute bias error
MBE	mean bias error
n	number of data points to be observed
RMSE	root mean square error
TSRY	typical solar radiation year
λ	site latitude (degree, °N)
ϕ	site longitude (degree, °E)

2. The development and validation of a simple polynomial model

The measuring work in the National Cheng Kung University in South Taiwan (Tainan, 23°N 120°E) provided the data of I_{global} and $I_{diffuse}$ from 1 January 2011 – 31 December 2012. The instruments used were pyranometer (Model PSP) and shadow band stand (Model SBS) of The Eppley Laboratory, Inc. [1]. The database was then examined by the checking method of Reindl et al. [2] and filtered by the moving average technique (size – 25) [3 – 4], in which a better regression model could be established given by Eq. (2).

$$d = 0.9823 \ , \qquad 0 \le k_t < 0.2$$
$$d = 0.8066 + 1.9651\ k_t - 6.5435\ k_t^2 + 3.8590\ k_t^3 \ , \qquad 0.2 \le k_t < 0.75 \qquad (2)$$
$$d = 0.2255 \ , \qquad k_t \ge 0.75$$

where k_t is the ratio of I_{global} to H_0. The parameters were determined using the least squares method (polyfit of MATLAB® [5] function). With the knowledge of k_t records, the hourly diffuse fraction could be estimated by a simple 3rd – order polynomial function.

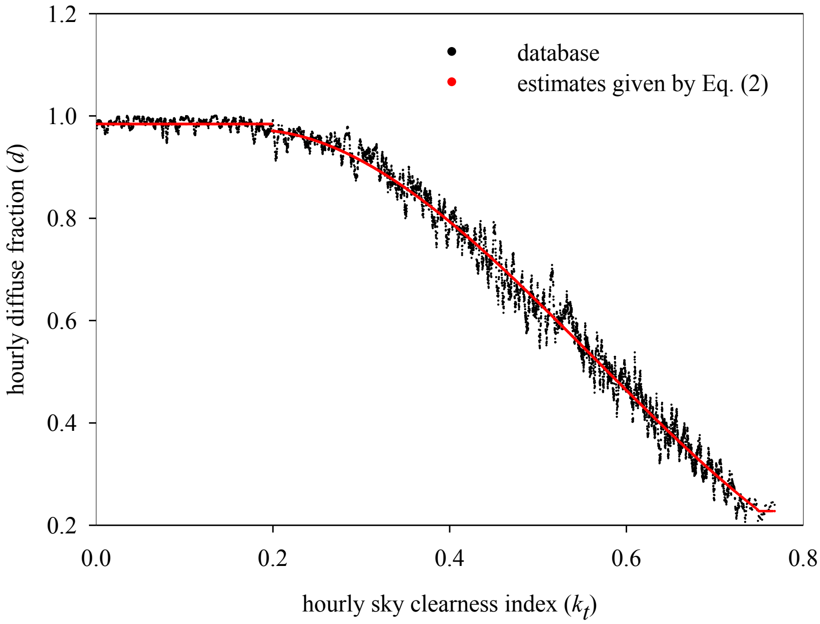

Fig. 1. Comparison of the $d - k_t$ data with those predicted using the proposed model

Fig. 1 shows a direct comparison between the model estimates and the filtered database, where good matches were observed. Next, two commonly used statistical indicators, the mean bias error (MBE) and the root-mean-square error (RMSE), were used to measure the model error against those of Reindl et al. [2], Miguel et al. [6], and Chandrasekaran and Kumar [7]. To confirm the generality of data comparison, the minutely integrated data collected by the High Concentration Photovoltaic R&D Project of Institute of Nuclear Energy Research in North Taiwan (Taoyuan, 25°N 121°E) in 2008, were also introduced in the error analysis. Note the Taoyuan data sets were not included as model database since the instruments were not routinely calibrated, in which the measuring error were assumed to be higher than the case in South Taiwan. The locations of Tainan and Taoyuan were shown in Fig. 2.

Fig. 2. The Taiwan regional map

From Table 1, it was observed that the proposed model was of general validity for the Taiwan area. That of Chandrasekaran and Kumar [7] was the next best one demonstrating satisfactory performance. If the statistical results were interpreted, Eq. (2) provided an average amount of under-estimation at places not used in model development [8].

$$\mathrm{MBE}(\%) = \frac{100}{\overline{d}_{mea}}\left[\frac{1}{n}\sum_{i=1}^{n}\left(d_{est}-d_{mea}\right)\right] \tag{3}$$

$$\mathrm{RMSE}(\%) = \frac{100}{\overline{d}_{mea}}\left[\frac{1}{n}\sum_{i=1}^{n}\left(d_{est}-d_{mea}\right)^2\right]^{1/2} \tag{4}$$

Table 1. Statistical performance of the models considered, for Tainan and Taoyuan data sets

	Tainan (South Taiwan)		Taoyuan (North Taiwan)	
	MBE (%)	RMSE (%)	MBE (%)	RMSE (%)
Proposed model, Eq. (2)	0.01	3.20	-2.42	4.00
Reindl et al. [2]	0.18	4.05	-3.46	5.02
Miguel et al. [6]	-0.29	3.95	-3.38	4.89
Chandrasekaran and Kumar [7]	0.03	4.01	-3.50	4.91

3. Creation of the updated typical solar radiation year data sets

To account for the climatic changes in the last decade, an updated typical solar radiation year (TSRY) was needed. Following the Sandia method ([9 – 11]), which was an empirical approach to select 12 typical months (January to December) from different years in the observation period, the updated TSRY which contained 8760 I_{global} records from the 2002 – 2011 was created. The 20 major meteorological stations of the Taiwan Central Weather Bureau provided the weather records shown in Table 2. Table 3 indicates of which particular year from the 10 – year period was selected in generating the updated TSRY data set.

Table 2. List of 20 major meteorological stations used in the creation of updated TSRY

	Elevation above sea level (km)	Latitude (°N)	Longitude (°E)
Keelung	0.0267	25.13	121.72
Anbu	0.8258	25.18	121.52
Zhuzihu	0.6071	25.15	121.53
Taipei	0.0053	25.03	121.50
Hsinchu	0.0269	24.82	121.00
Taichung	0.0840	24.13	120.67
Wuqi	0.0072	24.25	120.50
Sun Moon Lake	1.0148	23.87	120.88
Alishan	2.4134	23.50	120.80
Yushan	3.8448	23.48	120.95
Chiayi	0.0269	23.48	120.42
Yongkang	0.0081	23.03	120.22
Kaohsiung	0.0023	22.57	120.30
Hengchun	0.0221	22.00	120.73
Yilan	0.0072	24.60	121.73
Su-ao	0.0250	24.60	121.85
Hualien	0.0161	23.97	121.60
Chenggong	0.0335	23.08	121.35
Taitung	0.0090	22.75	121.13
Dawu	0.0081	22.35	120.88

Table 3. The years selected in generating the updated TSRY, using the 2002–2011 I_{global} records

	Jan	Feb	Mar	Apr	May	Jun	Jul	Aug	Sep	Oct	Nov	Dec
Keelung	2003	2004	2010	2011	2009	2011	2011	2011	2011	2002	2002	2008
Anbu	2003	2004	2008	2011	2009	2003	2004	2003	2003	2003	2002	2010
Zhuzihu	2011	2011	2011	2011	2002	2011	2011	2011	2002	2002	2002	2002
Taipei	2003	2004	2008	2011	2008	2003	2003	2003	2009	2003	2004	2010
Hsinchu	2010	2004	2005	2003	2004	2004	2003	2003	2009	2006	2004	2010
Taichung	2007	2009	2010	2009	2009	2011	2007	2006	2005	2007	2007	2007
Wuqi	2004	2003	2003	2004	2004	2004	2005	2003	2003	2011	2011	2011
Sun Moon Lake	2009	2004	2008	2004	2004	2003	2004	2006	2005	2003	2003	2008
Alishan	2009	2009	2010	2010	2004	2011	2003	2011	2005	2004	2004	2003
Yushan	2006	2004	2004	2004	2004	2004	2007	2009	2009	2006	2005	2003
Chiayi	2009	2009	2010	2011	2009	2011	2010	2008	2009	2008	2008	2008
Yongkang	2008	2007	2008	2007	2011	2011	2007	2011	2011	2011	2006	2007
Kaohsiung	2009	2003	2008	2007	2004	2004	2003	2011	2006	2003	2007	2010
Hengchun	2010	2010	2011	2011	2010	2011	2010	2010	2009	2010	2009	2009
Yilan	2007	2003	2010	2011	2004	2011	2011	2003	2010	2006	2005	2010
Su-ao	2003	2003	2005	2004	2004	2004	2004	2003	2005	2005	2005	2008
Hualien	2009	2007	2010	2004	2004	2007	2007	2004	2004	2006	2003	2008
Chenggong	2009	2004	2010	2003	2010	2009	2004	2010	2009	2004	2009	2003
Taitung	2009	2006	2009	2003	2004	2004	2003	2004	2003	2003	2005	2010
Dawu	2009	2011	2003	2011	2004	2011	2003	2011	2003	2006	2005	2004

It was worth-noting that the I_{global} records in the TSRY data sets had to be at intervals of solar time, accounting for the time shift among places of different longitude. To investigate the improvements made by this correction, the mean absolute bias error (MABE) of k_t was calculated given by Eq. (5), which was 1.0%. This indicated that the short range of longitude of Taiwan (2°) made the use of local time acceptable.

$$\text{MABE}(\%) = \frac{100}{\overline{k_t^{'}}}\left(\frac{1}{n}\sum_{i=1}^{n}\left|k_t - k_t^{'}\right|\right) \tag{5}$$

where $k_t^{'}$ is the corrected k_t value at intervals of solar time; $\overline{k_t^{'}}$ was the mean of $k_t^{'}$

4. Regression between monthly diffuse fractions and geographical parameters of places

To produce diffuse fraction maps showing distributions, a different approach was required since the full collections of I_{global} records were cumbersome and costly. It was the regression between monthly diffuse fractions of 20 major stations and their geographic parameters (latitude, longitude, and elevation above sea level). In an effort to find the best ones, Eqs. (6) – (8) in linear formats were discussed.

$$d_{mon} = x_{11}\ \lambda + x_{12}\ \phi + x_{13}\ h \tag{6}$$

$$d_{mon} = x_{21}\ \lambda + x_{22}\ h \tag{7}$$

$$d_{mon} = x_{31}\ \phi + x_{32}\ h \tag{8}$$

where d_{mon} was the monthly averaged diffuse fraction given by Eq. (9).

$$d_{mon} = \frac{\sum_{j=1}^{day}\left[\left(\sum_{i=1}^{24} I_{global}\right)\times d_{day}\right]}{\sum_{j=1}^{day}\left(\sum_{i=1}^{24} I_{global}\right)} \tag{9}$$

where day was the number of day in a month; d_{day} was the daily averaged diffuse fraction given by Eq. (10).

$$d_{day} = \frac{\sum_{i=1}^{24}\left(d_{est}\times I_{global}\right)}{\sum_{i=1}^{24} I_{global}} \tag{10}$$

The hourly estimates were provided by the validated model using updated TSRY data sets at solar time intervals. In order to reduce the measuring inaccuracy affected by low solar radiation intensities, the total daily and monthly global radiations records were used as weight factors. The observation time periods were from the sunrise – sunset and 0900 – 1500 each day, for understanding the conditions under low-to-middle and high k_t skies, respectively.

Applying the ranking approach of Elagib and Mansell [12] to Eqs. (6) – (8), the use of latitude and elevation above sea level was found to have the best performance shown in Table 4, in which an increasing proportion of monthly diffuse fraction at higher latitude was observed. This could be attributed to the effect of averaged air mass variations with latitude in Taiwan that exhibited limited differences in ground reflectivity [13]. Table 4 also indicates that monthly value would increase for places at higher elevation in May – September while decreasing in other months. It may be explained by the typical rainy period from May – September in Taiwan and the study in solar radiation intensity with elevation by Becker and Boyd [14].

Table 4. The best performing linear regressions for d_{mon}

sunrise – sunset	0900 – 1500

Jan	$0.0238\ \lambda - 0.0588\ h$	$0.0224\ \lambda - 0.0546\ h$
Feb	$0.0224\ \lambda - 0.0556\ h$	$0.0208\ \lambda - 0.0497\ h$
Mar	$0.0240\ \lambda - 0.0356\ h$	$0.0224\ \lambda - 0.0286\ h$
Apr	$0.0237\ \lambda - 0.0246\ h$	$0.0221\ \lambda - 0.0162\ h$
May	$0.0215\ \lambda + 0.0020\ h$	$0.0199\ \lambda + 0.0146\ h$
Jun	$0.0207\ \lambda + 0.0005\ h$	$0.0191\ \lambda + 0.0119\ h$
Jul	$0.0182\ \lambda + 0.0294\ h$	$0.0166\ \lambda + 0.0452\ h$
Aug	$0.0193\ \lambda + 0.0261\ h$	$0.0179\ \lambda + 0.0363\ h$
Sep	$0.0197\ \lambda + 0.0097\ h$	$0.0184\ \lambda + 0.0228\ h$
Oct	$0.0199\ \lambda - 0.0304\ h$	$0.0186\ \lambda - 0.0192\ h$
Nov	$0.0212\ \lambda - 0.0426\ h$	$0.0201\ \lambda - 0.0389\ h$
Dec	$0.0218\ \lambda - 0.0638\ h$	$0.0206\ \lambda - 0.0589\ h$

Table 5 gives the MBE and RMSE values. The MBE did not differentiate the regression performances, while the RMSE indicated a better assessment in the sunrise – sunset observation. It was thus inferred that there existed a smaller even scatter about the line of sunrise – sunset estimation.

Table 5. Error analysis through the MBE and RMSE tests

	sunrise – sunset		0900 – 1500	
	MBE(%)	RMSE(%)	MBE(%)	RMSE(%)
Jan	0.37	15.05	0.14	17.31
Feb	0.08	10.61	0.07	12.43
Mar	0.14	10.44	0.10	12.08
Apr	-0.13	8.40	0.22	9.91
May	0.06	17.34	0.15	20.17
Jun	0.22	15.38	0.06	17.74
Jul	0.16	15.00	0.08	17.29
Aug	0.14	17.08	0.16	19.48
Sep	0.05	17.05	0.15	18.63
Oct	-0.24	11.86	-0.31	12.97
Nov	-0.15	13.38	-0.05	14.59
Dec	-0.17	11.68	0.03	12.81

5. Output maps

Using the linear interpolation method (griddata of MATLAB® function) with a 1-km uniform grid and regressions in Table 4, the diffuse fraction maps possessing goodness-of-fit surfaces could be produced. As shown in Fig. 3 (a) and (b), the 579 meteorological stations with listed spatial coordinates provided mapping information.

(a)

(b)

Fig. 3. The information of stations in (a) distribution; (b) geographic classification [15]

Fig. 4 (a) and (b) give the mapping results for two observation periods (the sunrise – sunset and 0900 – 1500). It was seen that in May and June, the diffuse fraction distributions for low-to-middle k_t ranges were not strongly affected by the site elevation. This could be resulted by the significance of solar altitude under clear skies [16]. If the monthly values were investigated in geographic perspective, they were decreasing in plain areas for January – June while increasing for July – December. The trend was inversed for the mountain regions. These may be contributed by the seasonal changes of solar radiation intensity, and the stronger effect of relative humidity on partly cloudy skies [2], respectively. As for those in March and April exhibiting higher values than February, the ample precipitation of Southwest Monsoons in Asia may be the explanation. In addition, if the yearly values were observed from Fig. 5 (a) and (b), the Southeast Taiwan had the largest potential for concentrating solar thermal system installations. On the other hand, the North Taiwan had the least utilization opportunity.

(a)

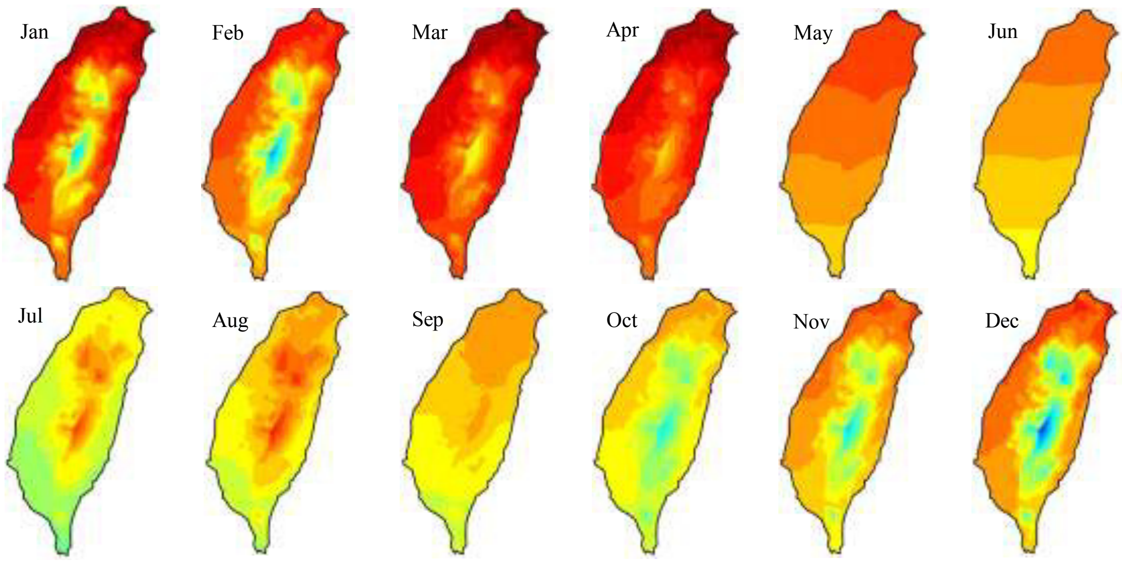

(b)

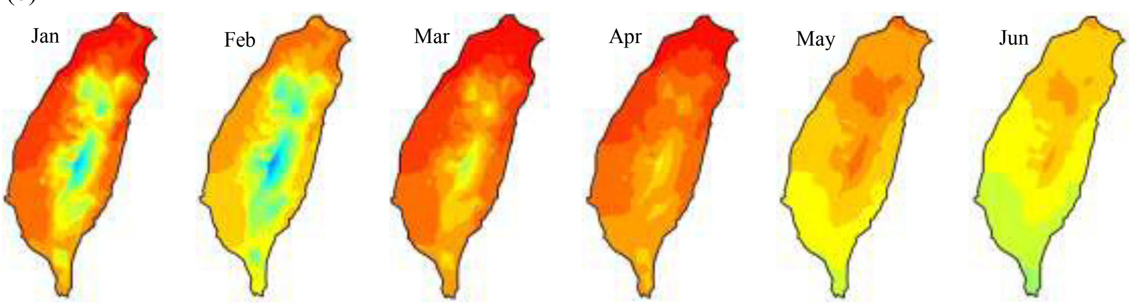

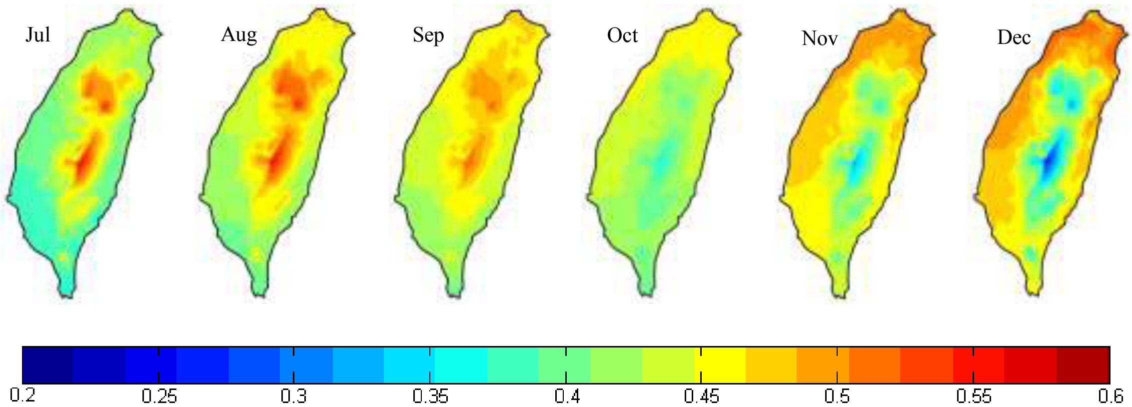

Fig. 4. The diffuse fraction maps showing monthly distributions, estimated from (a) sunrise – sunset; (b) 0900 – 1500 each day

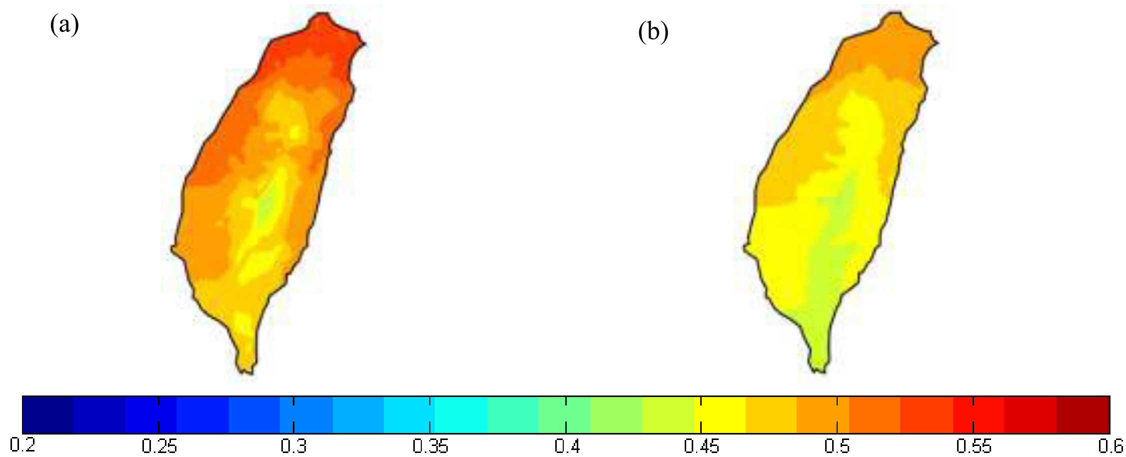

Fig. 5. The maps showing yearly conditions for the (a) sunrise – sunset; (b) 0900 – 1500

Since the satellite data of diffuse radiation were limited, the mapping reliability could not be accessed by means of error analysis. As a future work, a stochastic expression may be used by introducing uncertainty through the monthly diffuse fractions. Based on this approach, the mapping accuracy in any location and any month of the year could be well described without the knowledge of satellite data.

6. Conclusion

The polynomial model proposed in this paper was confirmed to be of general validity for the Taiwan area through the MBE and RMSE tests. Applying the model to the updated TSRY data sets contained I_{global}, the linear regression between monthly conditions and geographical parameters of places were discussed, in which the use of latitude and elevation above sea level were found to have the best performance. Next, diffuse fraction maps showing monthly and yearly distributions for the sunrise – sunset and the 0900 – 1500 observation periods were presented. It was concluded that the Southeast Taiwan was favorable to the concentrating solar thermal system installations, while the North Taiwan had the least opportunity.

Acknowledgements

This work was financially supported by the Bureau of Energy, the Ministry of Economic Affairs, Taiwan, Republic of China, under Grant No. 102 – D0304.

References

[1] The Eppley Laboratory, Inc. EPLAB. Available from http://www.eppleylab.com.

[2] Reindl DT, Beckman WA, Duffie JA. Diffuse fraction correlations. Sol Energy 1990;**45(1)**:1-7.

[3] Jacovides CP, Tymvios FS, Assimakopoulos VD, Kaltsounides NA. Comparative study of various correlations in estimating hourly diffuse fraction of global solar radiation. Renew Energ 2006;**31**:2492–2504.

[4] Torres JL, Blas M, Garcia A, Francisco A. Comparative study of various models in estimating hourly diffuse solar irradiance. Renew Energ 2010;**35**:1325–1332.

[5] MATLAB® - The Language of Technical Computing. Available from http://www.mathworks.com/products/matlab/.

[6] Miguel A, Bilbao J, Aguiar R, Kambezidis H, Negro E. Diffuse solar irradiation model evaluation in the north Mediterranean belt area. Sol Energy 2001;**70(2)**:143–153.

[7] Chandrasekaran J, Kumar S. Hourly diffuse fraction correlation at a tropical location. Sol Energy 1994;**53(6)**:505–510.

[8] Stone RJ. Improved statistical procedure for the evaluation of solar radiation estimation models. Sol Energy 1993;**51(4)**:289-291.

[9] Hall IJ, Prairie RR, Anderson HE, Boes EC. Generation of Typical Meteorological Years for 26 SOLMET Stations. SAND78-1601. Albuquerque, NM: Sandia National Laboratories, 1978.

[10] Marion W, Urban K. Users Manual for TMY2s-Typical Meteorological Years Derived from the 1961–1990 National Solar Radiation Data Base. NREL/TP-463-7668. Golden, CO: National Renewable Energy Laboratory, 1995.

[11] Wilcox S, Marion W. Users Manual for TMY3 Data Sets. NREL/TP-581-43156. Golden, CO: National Renewable Energy Laboratory, 2008.

[12] Elagib NA, Mansell MG. New approaches for estimating global solar radiation across Sudan. Energ Convers Manage 2000;**41**:419-434.

[13] Spencer JW. A Comparison of methods for estimating hourly diffuse solar radiation from global solar radiation. Sol Energy 1982;**29(1)**:19-32.

[14] Becker CF, Boyd JS. Solar radiation availability on surfaces in the United States as affected by season, orientation, latitude, altitude and cloudiness. Sol Energy 1957;**1(1)**:13–21.

[15] Google Maps. Available from http://maps.google.com/.

[16] Skartveit A, Olseth JA. A model for the diffuse fraction of hourly global radiation. Sol Energy 1987;**38(4)**:271-274.